

Petrochemistry of Mafic Granulite Xenoliths from the Chantaburi Basaltic Field: Implications for the Nature of the Lower Crust beneath Thailand

PRINYA PROMPRATED,¹ LAWRENCE A. TAYLOR,

Planetary Geosciences Institute, Department of Geological Sciences, University of Tennessee, Knoxville, TN 37996

AND CLIVE R. NEAL

Department of Civil Engineering and Geological Sciences, University of Notre Dame, Notre Dame, IN 46556

Abstract

Mafic granulite-facies xenoliths in alkali basalts from Chantaburi province represent the only known lower-crustal material in Thailand. Most xenoliths contain garnet (or its secondary product—kelyphite), plagioclase, and clinopyroxene, ± traces of corundum, and are grouped into garnet-rich and clinopyroxene-rich granulites (Groups 2 and 3, respectively). One sample is classified as olivine-garnet clinopyroxenite (Group 1), reflecting the presence of olivine and spinel and the absence of plagioclase. Whole-rock chemistry suggests that the protoliths of these granulite xenoliths have high normative olivine, plagioclase, and diopside, and, in most cases, low abundances and generally flat REE profiles with positive Eu anomalies. These characteristics indicate that the protoliths originated as basaltic cumulates, similar to troctolite and olivine-gabbro. On cooling, cumulate protoliths transformed to granulite-facies assemblages, mainly by the reaction: $Pl + Ol = Gt + Cpx$. Interestingly, some granulite xenoliths contain corundum, interpreted as a product of incongruent melting of plagioclase, that may have crystallized sometime prior to the complete transformation of protoliths to garnet granulites. P-T estimates indicate that the xenoliths last equilibrated at ~1100 to 1200°C and 15 to 18 kbar, consistent with depths around 50 to 60 km. The occurrence of mafic granulite xenoliths in Thailand may indicate prolonged periods of basalt underplating that generated new lower crust, and eventually culminated with Late Cenozoic alkali basalt volcanism.

Introduction

KNOWLEDGE OF THE lower continental crust has been significantly improved through studies of granulite-facies rocks, emplaced at the Earth's surface either as massive terrains or as xenoliths in alkali basalts and kimberlites. As generally observed, granulite-facies terrains tend to have intermediate to felsic compositions, whereas granulite xenoliths are predominantly mafic (e.g., Griffin and O'Reilly, 1986; Rudnick, 1992; Rudnick and Fountain, 1995). Furthermore, in terms of crustal provenance, granulite-bearing alkali basalts typically occur in non-cratonic regions within Proterozoic to Phanerozoic crustal blocks, in contrast to granulite-bearing kimberlites and granulite terrains that are more common in Archean cratons (Rudnick, 1992).

Many Cenozoic alkali basalts in Asia contain granulite xenoliths, from which information on the

nature of lower continental crust in this region has been obtained. For instance, based on compositions of two-pyroxene and garnet granulites, Stosch et al. (1995) suggested that the lower crust in Mongolia is broadly basaltic to andesitic, and probably was derived from fractionated melts or cumulates from such compositions. Their P-T estimates, derived from garnet granulites, yield 14 kbar and 840°C. Kopylova et al. (1995) further concluded that the crust-mantle boundary of this region is located at about 45 km depth, implying a relatively thick crust. Similarly, in northern China, Liu et al. (2001) and Chen et al. (2001) determined the depth of the crust-mantle interface at 42 km, based on P-T estimations from granulite xenoliths in conjunction with P-wave velocities.

In Thailand, despite the occurrences of deep-seated materials such as mantle xenoliths and megacrysts in many Cenozoic alkali basalts, information on the lower continental crust from this Southeast Asian region is relatively unknown. Previously,

¹Corresponding author; email: prinya@utk.edu

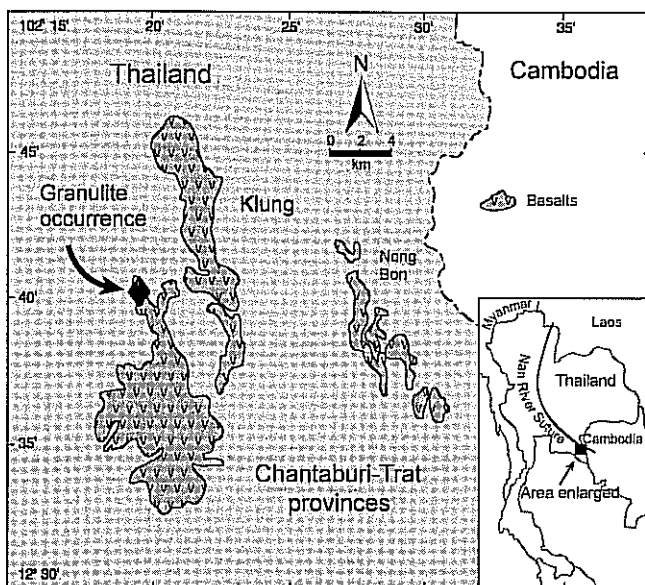


FIG. 1. Occurrence of granulite xenoliths in Thailand. Distributions of alkali basalts are from Vichit (1992).

petrochemical investigations were aimed at understanding the genesis of gem-quality corundum (ruby and sapphire) through studies of basalts, as well as inclusions in corundum megacrysts that occur abundantly in placer deposits near these basaltic fields (e.g., Vichit et al., 1978; Barr and MacDonald, 1981; Guo et al., 1996; Intasopa et al., 1999; Sutthirat et al., 2001; Limtrakun et al., 2001). Only a few studies have been performed on mantle-derived megacrysts and peridotite xenoliths (Barr and Dostal, 1986; Promprated et al., 1999).

Our efforts to understand the nature of the deep crust/upper mantle in this area have resulted in the recognition of rare granulite xenoliths that occur in alkali basalt flows of the Klung district, Chantaburi province (Fig. 1). This discovery represents a unique opportunity to constrain compositions of the lower continental crust in this region, as well as to understand the processes involved in its formation and modification. In the present investigation, we focus on major- and trace-element chemistry of the granulite xenoliths, and also address the formation of corundum in some of our samples.

General Geology and Samples

The Chantaburi-Trat alkali basalts occur as small hills of volcanic plug remnants and isolated

flows in an area roughly 30 × 70 km (Vichit, 1992); however, most basalts are extensively weathered and covered by thick basaltic soils. In places, basaltic flows overlie sedimentary rocks of Carboniferous to Permian age (Sivabovorn et al., 1976; Salyaphongse and Jungyusuk, 1983). Limited geochemical and radiometric data (K-Ar) indicate that these basalts are basanitoid or nephelinite, and were erupted within the last million years (Vichit et al., 1978; Barr and MacDonald, 1981). It is generally believed that the Late Cenozoic basalts of Thailand are the products of decompressional melting, possibly related to extensional rifting (Barr and MacDonald, 1978; Bunopas and Vella, 1992; Mukasa et al., 1996).

The basaltic flows in which granulite xenoliths occur are up to 15 m thick, and lie as deep as 30 m beneath the surface (Vichit, 1992). They were exposed and then disintegrated by gem-mining operations. It is unfortunate that outcrops of these granulite-bearing basalt flows could not be investigated, inasmuch as they have been under water since the cessation of mining. Nevertheless, a number of granulite xenoliths were collected from mining debris, 10 of which were used in the present investigation. They include 9 garnet granulites and a rare olivine-garnet clinopyroxenite. Most xenoliths are 5–8 cm across, with the largest approximately

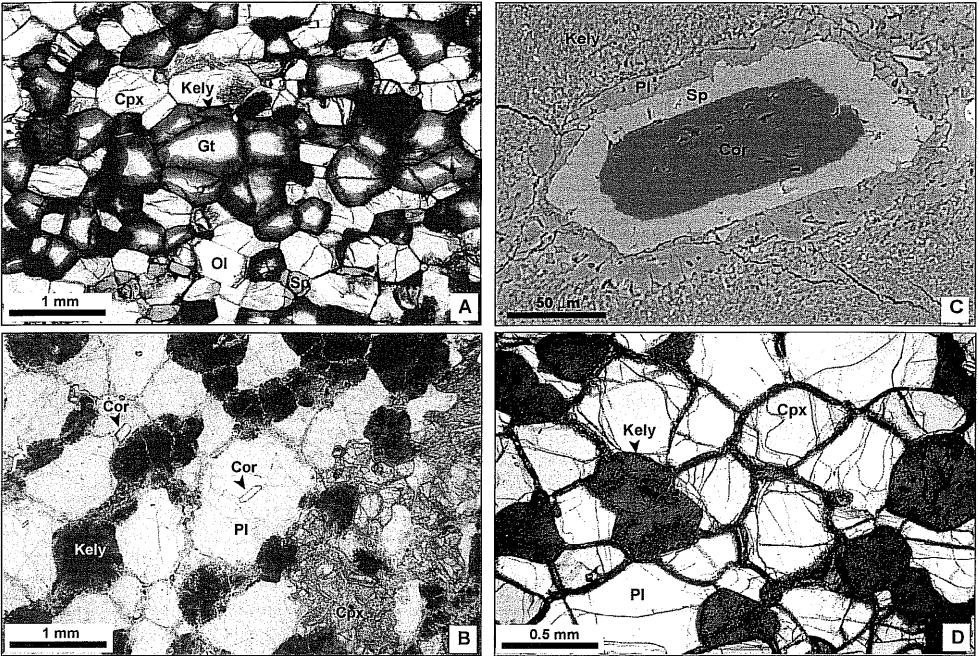


FIG. 2. A. Kelyphitic rims around garnet in olivine-garnet clinopyroxenite (KL9). The garnets also form crude layering. B. Corundum inclusions in plagioclase of garnet-rich granulite (KL10). Garnets are completely overprinted by kelyphite. C. Backscattered electron (BSE) image of a relic corundum inclusion in kelyphite (KL10). The corundum is replaced and mantled by an intermediate rim of spinel and an outer rim of plagioclase. D. Typical texture of clinopyroxene-rich granulite (KL7). Figures 2A, 2B, and 2D are in plane-polarized light; reflected light is also used in Figure 2D. Abbreviations: Gt = garnet; Kely = kelyphite; Cpx = clinopyroxene; Ol = olivine; Sp = spinel.

12 cm in diameter. As a suite, these xenoliths will be simply referred to as garnet granulites.

Petrography

The granulite xenoliths display granoblastic, equigranular, and polygonal texture, commonly with 120° triple-junction grain boundaries. Some samples also exhibit millimeter-scale banding. No stress features (i.e., kink bands) were observed. All major minerals—clinopyroxene (Cpx), plagioclase (Pl), and garnet (Gt)—are of similar size, ranging from 0.5 to 2.0 mm. However, large Cpx grains (up to 5 mm) also occur in most samples. Minor minerals include olivine (Ol; 0.5–1.0 mm), spinel (Sp; ~ 0.2 mm), and corundum (Cor; up to 300 μm). Based on mineralogy and chemistry, the samples can be broadly classified into three groups: (1) olivine-bearing garnet clinopyroxenite; (2) garnet-rich granulite, the most common type; and (3) pyroxene-rich garnet granulite.

Group 1: Olivine-garnet clinopyroxenite

Xenolith KL9, the only olivine-garnet clinopyroxenite in this collection (Table 1), exhibits well-defined banding mainly as discontinuous garnet trains. These garnets are moderately altered to brown, fibrous-like kelyphite, which is radially arranged as rinds around primary garnets (kelyphitic rims; Fig. 2A). This kelyphite is extremely fine grained ($\ll 1\mu\text{m}$) such that individual minerals cannot be resolved petrographically or by electron microprobe. In addition, garnets typically contain circular microcracks, which is a texture that has been interpreted as a product of decompression (Rudnick, 1992).

Clinopyroxenes are generally unaltered and lack exsolution lamellae. It is common, however, to find “spongy-textured rinds” developed along margins or cracks of Cpx. This reaction feature of Cpx consists mainly of secondary clinopyroxene and green spinel. According to Taylor and Neal (1989), spongy rims occur when Na and Al from primary

TABLE 1. Reconstructed Primary Modal Abundances of Granulite Xenoliths from Thailand¹

Sample	Cpx	Pl	Gt	Ol	Sp	Cor
Ol-Gt clinopyroxenite						
KL9	38.4	—	43.5	14.6	3.5	—
Gt-rich granulite						
KL12	39.4	29.6	31.0	—	—	—
KL4a	21.3	27.9	50.8	—	—	—
KL11	19.5	21.4	59.1	—	—	—
KL5	17.2	27.7	55.1	—	—	Inc ³
KL13	23.6	23.9	52.5	—	—	Inc
KL10	22.2	39.4	36.0	—	2.4 ²	Inc
KL14	27.7	45.8	26.5	—	—	—
Cpx-rich granulite						
KL8	43.7	28.7	27.6	—	—	—
KL7	44.3	27.3	28.4	—	—	—

¹Determined by point counting approximately 3000–5000 points per thin section. Kelyphite was counted as primary garnets. Abbreviations: Cpx = clinopyroxene; Pl = plagioclase; Gt = garnet; Ol = olivine; Sp = spinel; Cor = corundum.

²Secondary spinel.

³Corundum occurs as inclusions in the sample.

clinopyroxene are effectively “leached” by metasomatic fluids during a melting process. The consequence of this is the volume decrease that results in cracking of the clinopyroxene, but without disrupting the optical continuity of the margins and core. Snyder et al. (1997a) explained this texture in lherzolite xenoliths from China by the reaction: Cpx₁ + K-rich fluids = Cpx₂ + alkali feldspar ± sulfide ± titanomagnetite.

Olivines are typically subhedral tabular, with minor alteration to serpentine. A few spinels occur interstitially, probably as the last mineral to crystallize.

Group 2: Garnet-rich granulite

The majority of the granulite xenoliths belong to this group (Table 1), and contain garnet or plagioclase in significantly greater abundance than clinopyroxene. The Cpx-rich xenolith KL12 is included in this group because its mineral chemistry (see below) is similar to that of Gt-rich samples. Generally, clinopyroxenes and plagioclases are unaltered, except for KL10 where clinopyroxenes are extensively metasomatized to secondary Cpx and Sp. Garnets characteristically contain circular cracks, and are extensively or completely overprinted by dark

brown, turbid, kelyphite. Apparently, the initial nucleation of garnets occurred at Pl-Pl or Pl-Cpx grain boundaries. Fine banding due to contrasting proportions of minerals is present in some samples. In KL14, Cpx grains form lenticular aggregates that enhance the overall layering appearance. Some Cpx aggregates contain interstitial K-rich feldspathic glasses, possibly a product of late-stage metasomatism.

Samples KL5, KL13, and KL10 are particularly interesting because they contain corundum as inclusions in plagioclases or kelyphitized garnets (Figs. 2B and 2C). These inclusions are generally euhedral to subhedral prismatic (up to 300 µm), and some are trigonal in cross section. The occurrence of corundum inclusions in the relatively unaltered xenolith KL13 suggests that their origin was not due to secondary processes that involved external melts/fluids. In the highly kelyphitized KL10, many corundum inclusions are mantled by rims of spinel, and, in some cases, corundum grains have intermediate rims of spinel and outermost rims of plagioclase (Fig. 2C). These rims possibly reflect the reaction of corundum with metasomatic fluids and/or kelyphite. In a few cases, a single corundum grain appears to grow into adjacent plagioclase grains.

Group 3: Clinopyroxene-rich granulite

Clinopyroxene is the most abundant mineral (~44%; Table 1) in xenoliths KL7 and KL8 of this group. Unlike samples from the previous groups, granulites KL7 and KL8 show no obvious mineral banding (Fig. 2D). Garnets in both samples are completely kelyphitized, whereas clinopyroxene and plagioclase in KL7 remain relatively unaltered. Metasomatic-induced partial melting appears to have affected xenolith KL8, in which Cpx developed spongy rims consisting of secondary Cpx and Pl, with, in some cases, K-rich feldspathic glass, but without spinel. Partially melted plagioclases typically exhibit corroded rims, becoming more An-rich compared to the primary core.

Analytical Techniques

Major elements of minerals and whole-rock samples were determined with an automated CAMECA SX-50, four-spectrometer electron microprobe (EMP), at the University of Tennessee. Data were collected using a wavelength-dispersive technique and corrected using the PAP procedure. EMP analyses of whole-rock samples were performed on fused glass beads, which were prepared by fusing sample powders on molybdenum-strip heaters under a nitrogen atmosphere (Jezek et al., 1978). Instrumental conditions for glass-bead analyses employed an accelerating potential of 15 kV, an electron beam of 20 nA with a beam size of 20 or 30 μm , and 20 s counting times for all elements. For mineral analyses, similar analytical conditions were used, but with a 30 nA beam current and a 5 μm beam size. Broad-beam analyses of the "bulk" kelyphite were performed with a 30 nA electron beam at 10 μm .

Whole-rock trace-element concentrations were obtained with a FISIONS-VC Elemental PlasmaQuad II inductively coupled plasma mass spectrometer (ICP-MS) at the University of Notre Dame. Samples were dissolved in ultrapure HF/HNO₃ acids in a clean 1000 class lab. Approximately 50 mg of powder from each sample was dissolved. Reference material BHVO-1 was also analyzed with the granulite xenoliths and host basalt. Details of the ICP-MS analytical conditions and procedures can be found in Neal (2001).

Whole-Rock Chemistry

Representative samples of all three xenolith groups and a host basalt were analyzed for major

and trace elements (Tables 2 and 3). Based on the major-element chemistry, all granulite xenoliths analyzed are mafic (~43–49 wt% SiO₂), similar to hypersthene-olivine normative tholeiitic or nepheline-olivine normative alkali-basaltic magmas. With lower SiO₂ but higher alkali contents, the host basalt (KLbs11) is classified as basanite, consistent with basalts from surrounding areas (Mukasa et al., 1996).

In major-element variation diagrams (Figs. 3A–3D), MgO is negatively correlated with SiO₂ and Na₂O+K₂O. In plots of MgO against Al₂O₃ and CaO (Figs. 3B and 3C), the two Cpx-rich samples (KL8 and KL12) appear to follow the arrays formed by the more evolved granulite xenoliths from Chudleigh (Australia) and Mongolia (Rudnick et al., 1986 and Stosch, et al., 1995, respectively). Compositions of the host basalt are significantly distinct from those of granulite xenoliths, suggesting no genetic relationship between them (Figs. 3A–3D).

Trace-element concentrations in the granulite xenoliths also vary systematically with MgO (Fig. 4). For instance, the compatible element Ni correlates positively with MgO, as expected when olivine is a crystallizing phase. This in turn results in negative correlations with the moderately and highly incompatible elements such as Zr, Hf, and La. The olivine-garnet clinopyroxenite (KL9) is relatively depleted in incompatible elements and deviates from negative trends formed by the garnet granulite xenoliths. This possibly reflects the greater abundance of olivine in the protolith of KL9 compared to that of other samples. For highly incompatible elements, Ba concentrations vary in a limited range. In contrast, Th exhibits more variation and is elevated in some samples compared with the well-defined negative trend of the Chudleigh data.

Chondrite-normalized (Anders and Grevesse, 1989) rare-earth element (REE) patterns are generally flat, although light REE (LREE) enrichments are present in a few samples (Fig. 5). All but sample KL12 show positive Eu anomalies (Eu/Eu* up to 3.4, where Eu* is the interpolated value between Cl-normalized Sm and Cd abundances), suggesting plagioclase accumulation. Note that the olivine-garnet clinopyroxenite, KL9, which lacks plagioclase, also displays a positive Eu anomaly. Finally, KL9 contains the lowest REE contents, whereas KL8 contains the highest, consistent with the former being most primitive and the latter most evolved among the samples in this study.

TABLE 2. Whole-Rock Compositions and CIPW Normative Mineralogy of Granulite Xenoliths and Host Basalt

Sample:	KL9	KL5	KL13	KL4	KL12	KL10	KL8	KLbs11 (basalt)
Whole-rock compositions, wt% ¹								
SiO ₂	43.1	44.8	45.0	45.7	48.1	45.9	48.6	42.2
TiO ₂	0.09	0.08	0.13	0.09	0.23	0.19	0.45	3.00
Al ₂ O ₃	16.9	21.4	21.4	20.9	18.2	22.1	17.2	13.1
Cr ₂ O ₃	0.06	<0.03	0.07	0.07	0.18	0.03	0.07	<0.03
MgO	18.8	13.1	12.3	11.7	10.5	10.1	9.18	9.96
CaO	9.49	11.1	12.0	12.0	14.0	11.5	12.0	9.71
MnO	0.12	0.08	0.10	0.09	0.08	0.08	0.13	0.16
FeO	7.49	4.99	4.96	5.37	4.28	5.08	6.73	11.0
NiO	0.04	n.a. ⁴	n.a.	n.a.	n.a.	n.a.	n.a.	0.04
Na ₂ O	1.07	1.33	1.43	1.54	2.12	2.24	2.76	3.65
K ₂ O	0.09	0.47	0.30	0.13	0.16	0.45	0.72	2.18
P ₂ O ₅	<0.03	<0.03	<0.03	<0.03	0.03	0.06	0.03	0.72
LOI ²	2.49	2.28	2.10	2.34	1.83	1.98	1.23	2.34
Total	99.81	99.72	99.90	99.90	99.64	99.73	99.11	98.00
Mg# ³	81.8	82.4	81.6	79.5	81.4	78.0	70.8	61.9
CIPW normative mineralogy (%) ⁵								
Qtz	0	0	0	0	0	0	0	0
Cor	0	0	0	0	0	0	0	0
Or	0.53	2.77	1.77	0.77	0.94	2.66	4.25	12.87
Ab	9.04	11.24	11.98	13.02	16.26	15.27	19.16	2.64
An	41.02	51.01	51.06	49.71	39.65	48.90	32.40	12.92
Ne	0	0	0.06	0	0.90	1.99	2.26	15.29
Di	4.69	3.09	6.64	7.70	23.58	6.21	21.72	24.78
Hy	1.24	1.84	0	3.89	0	0	0	0
Ol	39.07	26.29	24.94	21.29	15.10	21.25	15.86	17.81
Mt	1.42	0.95	0.94	0.97	0.81	0.96	1.28	2.08
Ilm	0.17	0.15	0.25	0.17	0.44	0.36	0.86	5.71
Ap	0	0	0	0.05	0.06	0.12	0.06	1.56

¹Obtained from EMP analyses (average of 20–25 analyses) on fused glass beads.

²Loss on ignition: weight loss after heating a known amount of sample at 1000°C for 1 hr, and corrected for the oxidation from Fe²⁺ to Fe³⁺.

³Mg# = (100Mg/Mg + ΣFe).

⁴n.a. = not analyzed.

⁵Calculated using software Magma2 (Wohletz, 1996), assuming Fe₂O₃/FeO = 0.15. Mineral abbreviations: Cpx = clinopyroxene; Pl = plagioclase; Gt = garnet; Ol = olivine; Sp = spinel; Qtz = quartz; Cor = corundum; Ab = Albite; An = anorthite; Ne = nepheline; Di = diopside; Hy = hypersthene; Mt = magnetite; Ilm = ilmenite; Ap = apatite.

Mineral Chemistry

Clinopyroxene

The three xenolith groups are also defined by variations in clinopyroxene mineral chemistry

(Table 4 and Fig. 6). The most striking feature of the Cpx compositions is the high Al₂O₃ contents (~8–16 wt%) and associated low Na₂O (mostly <2 wt%). This corresponds to a higher proportion of Ca-Tschermak (CaTs) versus jadeite (NaAl^{vi}) molecules

TABLE 3. Trace-Element Analyses (ppm) of Selected Whole-Rock Granulite Xenoliths, Analyzed by ICP-MS

Sample:	KL9	KL5	KL13	KL4	KL12	KL10	KL8	BHVO-1	BHVO-1 ¹
Sc	6.2	5.5	11.5	11.7	27.3	7.3	34.3	31.7	31.8
V	18.5	15.6	37.3	42.2	90.5	27.4	201.9	307.2	317
Cr	343.6	121.5	358.1	394.4	960.5	64.6	422.3	289.8	289
Co	313.5	163.4	165.1	186.8	136.1	109.1	129.8	45.3	45
Ni	592.6	280.6	280.7	207.2	235.5	311.0	108.7	117.7	121
Cu	72.2	69.9	51.1	115.9	77.2	110.3	66.8	158.8	136
Zn	63.5	35.6	39.8	40.2	34.5	42.1	58.8	162.1	105
Ga	13.03	11.19	13.06	11.03	12.27	12.76	14.05	17.8	21
Rb	1.41	7.45	4.81	0.14	1.74	6.57	8.87	8.97	9.4
Sr	148.6	272.4	284.1	176.6	236.7	235.1	200.4	427.0	403
Y	1.02	1.36	2.86	1.95	4.09	2.22	9.20	21.7	24.4
Zr	2.91	2.69	5.00	2.94	9.58	10.46	13.57	171.3	179
Nb	8.35	3.88	3.32	3.44	4.74	4.93	4.42	19.4	19
Ba	3.31	37.17	20.6	17.1	23.0	37.3	54.4	134.2	139
La	0.37	0.33	0.40	0.44	1.39	2.21	1.60	15.9	15.8
Ce	0.93	0.90	1.15	1.04	2.94	4.62	3.88	41.3	39
Pr	0.12	0.15	0.18	0.13	0.37	0.56	0.56	5.51	5.7
Nd	0.59	0.79	1.00	0.62	1.74	2.28	2.89	25.8	25.2
Sm	0.18	0.28	0.31	0.19	0.49	0.46	0.96	6.44	6.2
Eu	0.10	0.27	0.21	0.29	0.16	0.24	0.48	2.14	2.1
Gd	0.21	0.39	0.53	0.34	0.76	0.52	1.60	6.77	6.4
Tb	0.03	0.04	0.07	0.06	0.11	0.07	0.25	0.97	0.96
Dy	0.22	0.30	0.51	0.34	0.66	0.42	1.62	5.41	5.2
Ho	0.03	0.06	0.10	0.07	0.14	0.09	0.33	1.03	0.99
Er	0.09	0.16	0.30	0.17	0.40	0.18	0.96	2.72	2.4
Tm	0.02	0.03	0.05	0.03	0.06	0.03	0.14	0.36	0.33
Yb	0.16	0.18	0.26	0.12	0.34	0.19	0.92	2.27	2.02
Lu	0.02	0.02	0.05	0.02	0.05	0.03	0.13	0.27	0.291
Hf	0.13	0.13	0.20	0.09	0.27	0.27	0.52	4.54	4.38
Pb	1.65	0.95	0.46	1.16	0.52	0.95	1.42	2.28	2.2
Th	0.07	0.02	0.04	0.02	0.19	0.31	0.25	1.32	1.22
U	0.05	0.02	0.02	0.01	0.09	0.08	0.09	0.42	0.42

¹Certified.

in clinopyroxenes from group 2 xenoliths, although the reverse is seen in clinopyroxenes from groups 1 and 3 (Table 4). In addition, the Al-rich nature is further accentuated by the presence of corundum in granulite xenoliths KL5, KL13, and KL10. Corundum is also present in xenoliths of similar compositions elsewhere (e.g., Beni Bousera: Kornprobst et al., 1990; Yakutia: Qi et al., 1997). Sample KL12 is unique; the whole-rock composition resembles that

of the Cpx-rich group, but compositions of Cpx are similar to the Gt-rich samples.

Two opposite trends of chemical zonation are also present in clinopyroxenes: (1) a gradual decrease in Al_2O_3 (up to ~0.5 wt%) in most xenoliths of groups 1 and 2; and (2) a sharp increase of Al_2O_3 up to ~3 wt% toward rims in KL14, KL7, and KL8 (Fig. 7). Na_2O and TiO_2 also follow the same zoning patterns as Al_2O_3 . Complimentary to

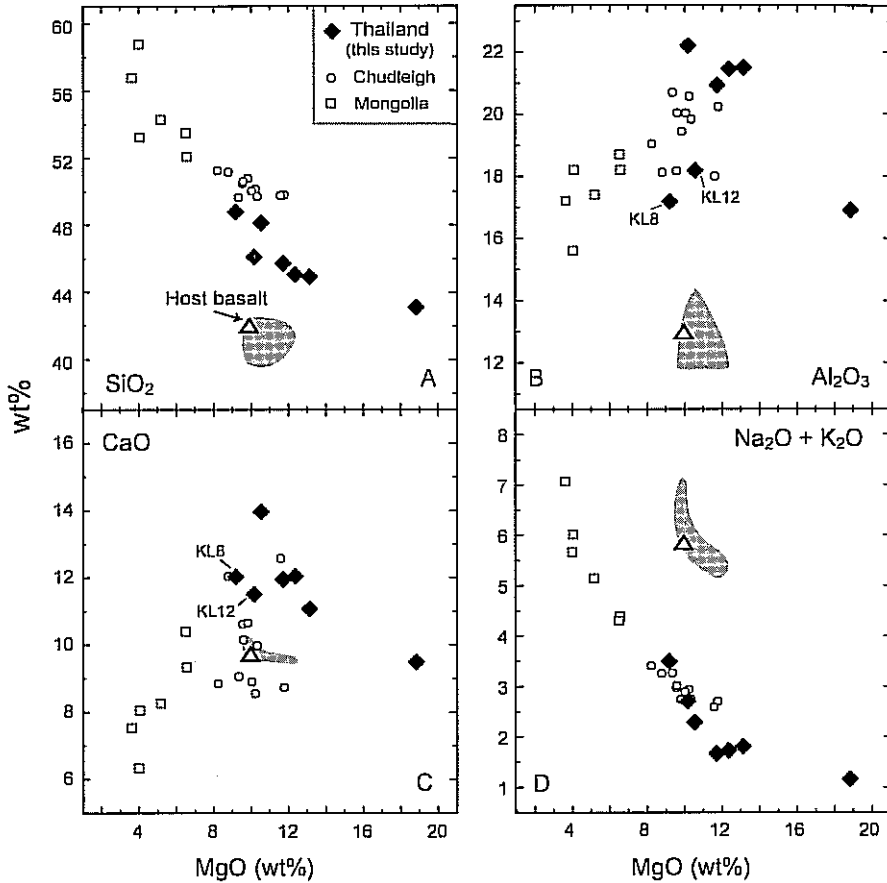


FIG. 3. Whole-rock compositions of the Thai granulite xenoliths, compared with granulite xenolith data from the literature (Chudleigh, Australia: Rudnick et al., 1986; Mongolia: Stosch et al., 1995). Well-defined negative trends of MgO versus SiO_2 and alkali content ($\text{Na}_2\text{O} + \text{K}_2\text{O}$) are suggestive of igneous fractionation. Samples KL8 and KL12 appear to follow the trends formed by more evolved xenoliths from the literature. The host basalt (open triangle) is compositionally distinct from—and may not be cogenetic with the granulite xenoliths. Shaded area represents compositions of basalts from nearby basaltic fields (Mukasa, 1996).

chemical gradients shown by these elements is the opposite zonation exhibited by MgO and SiO_2 , due to the coupled substitution: $\text{Si}^{(4)}\text{Mg}^{(6)} \leftrightarrow \text{Al}^{(4)}\text{Al}^{(6)}$. The slight decrease in Al toward the rims is typical of a cooling profile in Cpx (Loock et al., 1990; Pearson et al., 1995), whereas the significant increase in Al may reflect a period of subsequent reheating for some xenoliths.

Chemical heterogeneity is also observed within the spongy texture on Cpx rims. When compared with the primary Cpx (cores), the residual or secondary Cpx (rims) becomes depleted in Al_2O_3 and Na_2O , concomitant with the increase in MgO, CaO, and FeO contents (Table 4). Taylor and Neal (1989),

Snyder et al. (1997a), and Spetsius and Taylor (2002) interpreted this reduction of Al and Na in Cpx as the result of metasomatic-induced partial melting, assisted by the host basalts or kimberlites. In KL10, clinopyroxenes have core compositions similar to those of other Gt-rich granulites, but with rim compositions trending toward those of the Cpx-rich granulites.

Plagioclase

Plagioclase compositions range from generally labradorite (An_{54-61}) in the Gt-rich granulite to andesine (An_{35-41}) in the Cpx-rich xenoliths (Table 5), with slight variation in the orthoclase component

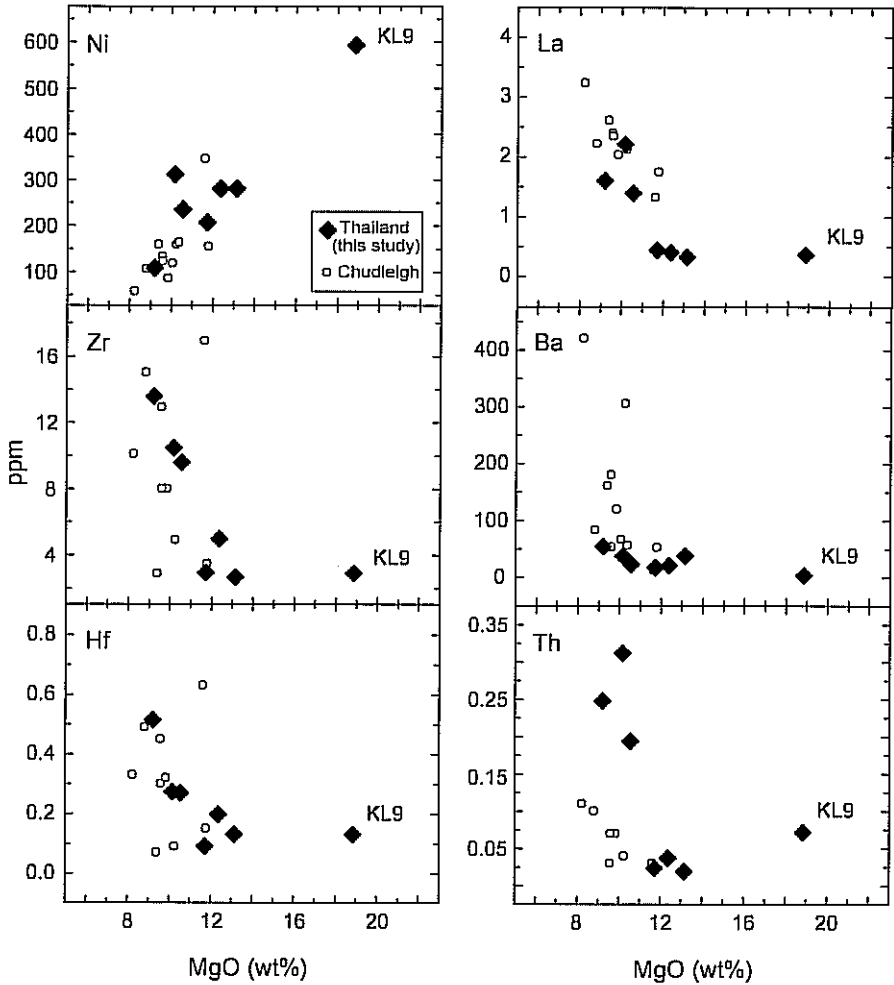


FIG. 4. Selected trace-element variations as a function of MgO contents in whole-rock granulite xenoliths. Igneous fractionation is suggested by the positive correlation with Ni, and by negative trends formed by incompatible trace elements (Zr, Hf, La, and Ba).

(Fig. 8). Plagioclase in most samples displays a slight compositional zonation, except in xenolith KL10 where it is considerably enriched in Na and K toward the rim, consistent with the highly metasomatized texture of this sample. In contrast, plagioclase in KL8 shows partially melted rinds along grain boundaries that leave "residual" plagioclase (Pl₂) with a substantial increase in anorthite contents (i.e., from An₃₆ at cores to An₆₆ at rims; Table 5). In the relatively fresh corundum-bearing samples (KL5 and KL13), there is also a slight increase in An content in the plagioclase rims (Fig. 8).

Garnet and kelyphite

All garnets have been subjected to variable degrees of kelyphitization; nevertheless, the compositions of either garnet remnants or kelyphite within a sample (shown as average analyses in Tables 6 and 7) are largely homogeneous at the grain scale. The relic garnet cores have pyrope components (Pyr) ranging from ~60 to 68 mol%, similar to those obtained from the bulk compositions of kelyphite. Note that Na₂O contents of kelyphite, although small, are detectable and indicate the introduction

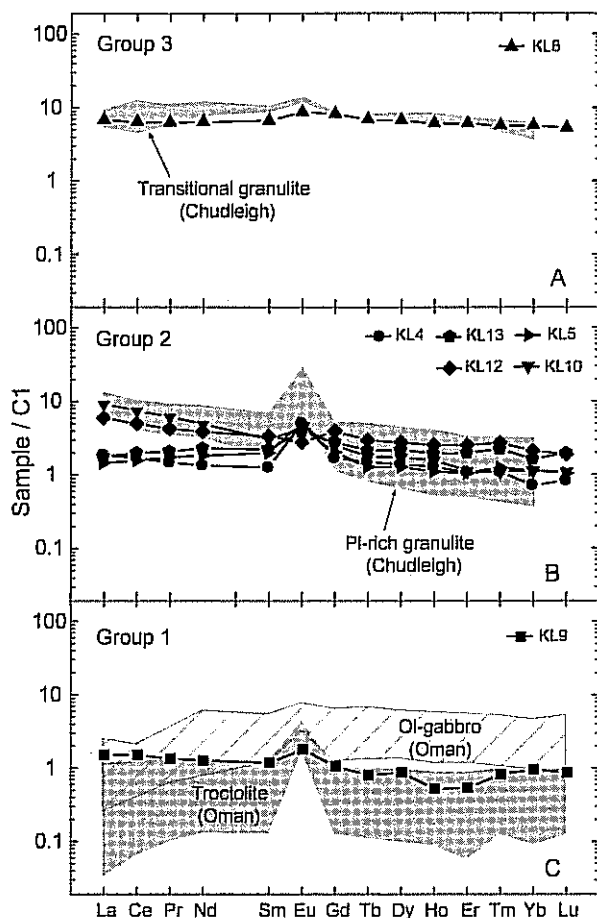


FIG. 5. Whole-rock REE profiles (chondrite normalized; Anders and Grevesse, 1989) of three granulite xenolith groups show general similarities with the Chudleigh granulite xenoliths (Rudnick et al., 1986) and the Oman ophiolite cumulates (Benoit et al., 1996). Positive Eu anomalies are observed in most samples, suggesting that plagioclase accumulation occurred in the protoliths.

of certain components outside garnet. In contrast, K_2O is undetected (<0.03 wt%).

Spinel

Two different compositional groups are present. (1) Primary spinels in the Ol-Gt clinopyroxenite have compositions similar to spinels that occur in the spongy rims of clinopyroxene (Table 8). Both have Mg# of approximately 77, with 0.3–0.4 wt% NiO and undetectable TiO_2 (<0.03 wt%). (2) Secondary spinels, which occur as rims around corundum inclusions, have lower Mg# (62) and NiO contents (0.14 wt%), but higher TiO_2 (0.13 wt%).

Olivine and corundum

The Fo content of olivines in the Ol-Gt clinopyroxenite (KL9) xenolith is ~86 (Table 9), which is slightly lower than that for olivines in a Thai wehrlite xenolith (~88) reported by Promprated et al. (1999). Corundum inclusions contain approximately 0.5–0.6 wt% Fe_2O_3 contents, noticeably higher than their Cr_2O_3 concentrations (0.03–0.20 wt%; Table 9). The amounts of these two elements fall within ranges obtained from some blue sapphire (Intasopa et al., 1999) and a Cpx-hosted corundum inclusion (Suthirat et al., 2001), recovered from the nearby basalt.

TABLE 4. Representative Compositions of Clinopyroxene in Granulite Xenoliths from Thailand¹

Sample:	KL9		KL12		KL1a		KL11		KL5		KL13	
	c	r	c	r	c	r	c	r	c	r	c	r
SiO ₂	52.2	52.7	49.1	49.9	48.1	48.7	48.1	48.2	47.2	47.5	47.3	47.6
TiO ₂	0.12	0.13	0.34	0.36	0.25	0.27	0.23	0.25	0.27	0.30	0.34	0.34
Al ₂ O ₃	9.10	8.78	11.4	10.7	12.2	11.5	13.1	12.8	14.4	14.1	14.5	14.1
Cr ₂ O ₃	0.07	0.03	0.35	0.25	0.31	0.10	0.21	0.19	0.27	0.16	<0.03	0.05
MgO	13.6	13.8	12.7	13.2	12.3	12.8	12.0	12.1	11.5	11.9	11.4	11.7
CaO	17.6	17.9	21.1	21.3	21.4	21.3	21.4	21.5	21.2	21.1	21.5	21.3
MnO	0.08	0.06	0.07	0.03	<0.03	<0.03	<0.03	0.03	<0.03	<0.03	0.04	0.04
FeO	3.52	3.68	2.92	2.73	3.08	3.14	2.98	3.05	2.58	2.60	2.52	2.74
Na ₂ O	2.84	2.74	1.45	1.41	1.32	1.23	1.52	1.49	1.69	1.64	1.53	1.51
Total	99.16	99.85	99.34	99.78	98.95	99.11	99.60	99.54	99.17	99.29	99.10	99.36
Cations based on 6 oxygens												
Si	1.890	1.896	1.790	1.808	1.764	1.782	1.752	1.756	1.723	1.731	1.725	1.734
Ti	0.003	0.004	0.009	0.010	0.007	0.007	0.006	0.007	0.007	0.008	0.009	0.009
Al	0.383	0.373	0.488	0.457	0.527	0.496	0.562	0.549	0.620	0.604	0.623	0.605
Cr	0.002	0.001	0.010	0.007	0.009	0.003	0.006	0.005	0.003	0.005	0.001	0.002
Mg	0.743	0.743	0.688	0.711	0.671	0.699	0.650	0.655	0.628	0.647	0.623	0.634
Ca	0.685	0.690	0.825	0.825	0.842	0.833	0.836	0.840	0.829	0.824	0.840	0.833
Mn	0.002	0.002	0.002	0.001	0.000	0.002	0.000	0.001	0.000	0.000	0.001	0.001
Fe	0.107	0.111	0.089	0.083	0.095	0.096	0.091	0.093	0.079	0.079	0.077	0.084
Na	0.199	0.191	0.103	0.099	0.094	0.087	0.107	0.105	0.120	0.116	0.108	0.107
Σ	4.010	4.011	4.004	4.001	4.009	4.005	4.011	4.011	4.014	4.014	4.007	4.009
Mg#	87.23	87.0	88.6	89.6	87.6	88.9	87.7	87.6	88.8	89.1	89.0	88.3
X _{jd}	0.199	0.191	0.103	0.099	0.094	0.087	0.107	0.105	0.120	0.116	0.108	0.107
X _{hats}	0.079	0.078	0.175	0.166	0.197	0.191	0.207	0.200	0.223	0.219	0.240	0.232
X _{hats+ti}	0.606	0.612	0.650	0.659	0.645	0.642	0.629	0.640	0.606	0.605	0.600	0.601
X _{en}	0.118	0.121	0.064	0.068	0.061	0.077	0.056	0.054	0.051	0.061	0.050	0.059

(continues)

TABLE 4. (continued)

Sample:	KL10	KL14	KL7	KL8	KL10	KL14	KL7	KL8	spgy
	c	f	c	f	c	f	c	f	
SiO ₂	47.1	48.2	48.0	46.9	50.0	50.2	50.0	49.7	50.7
TiO ₂	0.35	0.19	0.49	0.41	0.61	0.56	0.50	0.54	0.91
Al ₂ O ₃	15.8	15.1	12.0	15.1	8.86	10.8	9.46	11.1	2.88
Cr ₂ O ₃	0.03	<0.03	0.18	0.12	0.09	0.04	0.11	0.11	0.10
MgO	10.8	11.1	11.8	10.3	12.2	11.1	12.2	11.4	15.2
CaO	20.8	20.2	21.4	21.0	19.7	18.9	18.7	18.8	18.7
MnO	0.04	<0.03	0.04	0.04	0.08	0.07	0.09	0.06	0.21
FeO	2.78	3.03	4.01	3.96	5.86	5.52	5.79	5.83	10.0
Ni ₂ O	1.89	2.23	1.53	1.62	1.93	2.44	2.23	2.26	0.28
Total	99.62	100.10	99.36	99.52	99.35	99.58	99.15	99.71	99.02
Cations based on 6 oxygens									
Si	1.709	1.739	1.762	1.715	1.843	1.833	1.840	1.818	1.907
Ti	0.010	0.005	0.014	0.011	0.017	0.015	0.014	0.015	0.026
Al	0.677	0.642	0.517	0.651	0.384	0.467	0.411	0.477	0.128
Cr	0.001	0.000	0.005	0.003	0.003	0.001	0.003	0.003	0.003
Mg	0.584	0.597	0.647	0.562	0.671	0.605	0.667	0.619	0.851
Ca	0.810	0.781	0.840	0.823	0.777	0.738	0.744	0.734	0.755
Mn	0.001	0.001	0.001	0.001	0.003	0.002	0.003	0.002	0.007
Fe	0.084	0.091	0.123	0.121	0.180	0.169	0.178	0.178	0.316
Na	0.133	0.156	0.109	0.115	0.138	0.173	0.159	0.160	0.020
Σ	4.009	4.012	4.018	4.002	4.016	4.003	4.019	4.006	4.013
Mg#	87.4	86.8	84.0	82.3	78.9	78.2	78.9	77.7	
X _{jd}	0.133	0.156	0.109	0.115	0.138	0.173	0.159	0.160	
X _{calc}	0.253	0.225	0.170	0.251	0.089	0.127	0.092	0.135	
X _{hd+ti}	0.557	0.556	0.670	0.572	0.688	0.611	0.652	0.599	
X _{en}	0.056	0.066	0.050	0.056	0.082	0.082	0.097	0.099	

¹c, f, and spgy represent analyses at cores, rims, and spongy rim, respectively. K₂O contents of all analyses listed are <0.03 wt%.

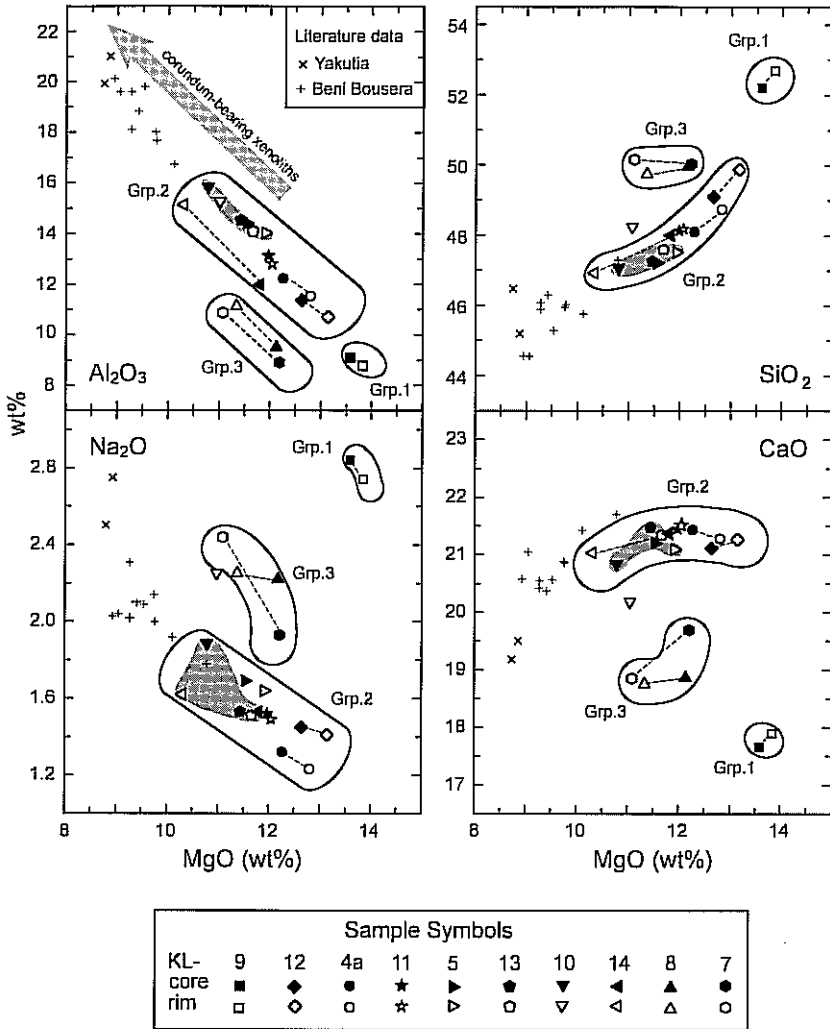


FIG. 6. Major-element compositions of representative core and rim analyses of clinopyroxenes in olivine-garnet clinopyroxenite (group 1), garnet-rich granulite (group 2), and pyroxene-rich granulite (group 3) xenoliths. Only selected tie lines that join between core and rim analyses of the same samples are shown for clarity. Envelopes represent the distribution of all analyses, with an exception for rim analysis of sample KL10 that may have been affected by metasomatism. Notice the higher Al_2O_3 in cores for group 1 and for the majority of group 2 xenoliths; the opposite is seen for group 3 and KL14 of group 2. Shaded fields encompass corundum-bearing samples in this study. The shaded arrow in the Al_2O_3 plot represents the Cpx compositions in mafic rocks that contain corundum, based on this study and data in the literature (Beni Bousera; Kornprobst et al., 1990; Yakulia; Qi et al., 1997).

Discussion

Origin of the granulite xenoliths

The systematic variations in whole-rock major and trace elements as a function of MgO suggest a genetic relationship among the granulite xenoliths

of the present study. Moreover, these granulite xenoliths were probably derived from basaltic-cumulate protoliths, based on the following rationale. First, the xenoliths exhibit simple mineralogy, mainly Cpx, Gt, and Pl, that can be produced by metamorphic reaction of basaltic cumulates (see below). This can be tested by calculating normative mineralogy

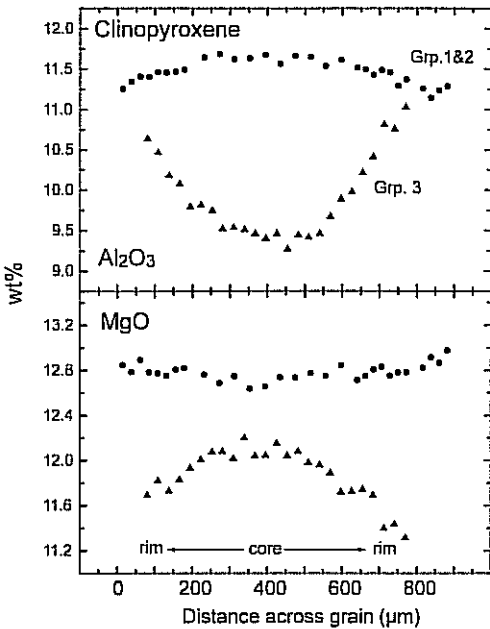


FIG. 7. Characteristic zoning profiles of clinopyroxenes of selected elements. Al_2O_3 contents in clinopyroxenes of groups 1 and 2 (with the exception of KL14) decrease toward rims, whereas MgO increases. More pronounced zonations in the opposite sense are seen in clinopyroxenes of group 3.

using the whole-rock compositions (an approach employed by Rogers and Hawkesworth, 1982 and Rudnick et al., 1986), and assuming that the granulite xenoliths have largely preserved their original protolith chemistry. This approach suggests that olivine, plagioclase, and diopside were present initially (Table 2) in protoliths such as troctolite and olivine gabbro. This interpretation is strengthened by REE patterns of the Thai granulite xenoliths that resemble those of the Oman troctolite and Chudleigh granulite xenoliths (Fig. 5), both of which contain textural evidence of igneous origins. Secondly, crystal fractionation causes significant variations in the concentration of compatible trace elements (e.g., Ni and Cr), whereas a small amount of fractionation only slightly affects the abundances of incompatible trace elements (e.g., La, Ba, and Th) in the cumulates, resulting in the low and relatively uniform abundances of these elements (Rudnick et al., 1986). These criteria are consistent with a significant variation in Ni contents (~109–593 ppm), but limited changes in the concentrations of incom-

patible elements (e.g., Zr, Hf, La, Ba, and Th; Fig. 4), as observed in this study.

The transformation of cumulate protoliths to garnet-bearing granulite-facies rocks has been suggested to occur during cooling from the initial igneous conditions, following the reaction: $\text{Pl} + \text{Ol} = \text{Cpx} + \text{Gt}$ (Harley, 1989; Pearson et al., 1991). In the present study, most samples contain Cpx, Pl, and Gt, except for KL9, in which Ol, Cpx, and Gt are present. Therefore, it is interpreted that, in most cases, olivine was less abundant and, hence, consumed by the reaction producing the assemblage of plagioclase, clinopyroxene, and garnet (or its secondary product—kelyphite). In contrast, plagioclase in clinopyroxenite KL9 appears to have been consumed first, resulting in the final assemblage with Ol, Cpx, and Gt. The occurrence of plagioclase in the protolith of KL9 is further supported by the preservation of a positive Eu anomaly in the whole-rock chemistry (Fig. 5). This feature has been previously reported in plagioclase-free garnet pyroxenites from Beni Bousera (Kornprobst et al., 1990).

Development of secondary texture: kelyphite and spongy rims

As noted above, alteration overprinting garnet in the Thai granulite-xenolith suite generally occurs as fine-grained or fibrous-like mineral aggregates or kelyphite. Typically, kelyphite is produced by: (1) metasomatic reaction between garnets and kimberlitic or basaltic magmas (Hunter and Taylor, 1982; Garvie and Robinson, 1984), or (2) the reaction of garnets with surrounding minerals such as olivine, pyroxenes, and plagioclase (Obata, 1994). Kelyphite produced by metasomatic processes usually exhibits an increase in K_2O , Na_2O , and $\text{H}_2\text{O} + \text{CO}_2$, compared with its garnet precursor (Hunter and Taylor, 1982). This results in the formation of a variety of mineral assemblages, including pyroxenes, plagioclase, spinel, phlogopite, amphibole, olivine, and K-rich glass (Taylor and Neal, 1989; Zang et al., 1993; Sobolev et al., 1994; Snyder et al., 1997a). In contrast, kelyphite formed by the reaction of garnet with adjacent pyroxene or plagioclase generally produces assemblages that contain orthopyroxene, spinel, plagioclase, olivine, and ilmenite (e.g., Kushiro and Yoder, 1966; Thompson, 1979; Rudnick, 1992; Obata, 1994).

In the Thai granulite xenoliths, kelyphite is extremely fine grained (<1 μm) such that the constituent minerals can only be analyzed in aggregate with an electron beam. The analyses show that

TABLE 5. Representative Compositions of Plagioclase in Granulite Xenoliths¹

Sample:	KL4a		KL13		KL5		KL11		KL12	
	c	r	c	r	c	r	c	r	c	r
SiO ₂	52.5	52.3	52.9	52.3	53.2	53.0	53.6	53.2	53.8	54.7
Al ₂ O ₃	29.6	29.3	29.1	29.4	28.9	29.1	28.7	28.7	28.7	29.1
CaO	12.4	12.6	12.0	12.3	11.5	11.7	11.6	11.7	11.2	11.3
FeO	0.07	0.16	0.03	0.08	0.07	0.12	0.05	0.16	0.05	0.13
Na ₂ O	4.35	4.16	4.59	4.21	4.96	4.73	5.03	4.64	5.22	4.91
K ₂ O	0.08	0.14	0.07	0.13	0.10	0.11	0.20	0.19	0.03	0.27
Total	98.92	98.65	98.67	98.56	98.74	98.86	99.23	98.65	98.94	100.40
Cations based on 8 oxygens										
Si	2.402	2.403	2.422	2.404	2.435	2.426	2.445	2.440	2.454	2.460
Al	1.595	1.587	1.573	1.594	1.560	1.571	1.543	1.551	1.541	1.540
Ca	0.606	0.619	0.589	0.607	0.565	0.575	0.565	0.576	0.546	0.543
Fe	0.003	0.006	0.001	0.003	0.003	0.005	0.002	0.006	0.002	0.005
Na	0.386	0.370	0.408	0.375	0.440	0.419	0.444	0.412	0.462	0.428
K	0.005	0.008	0.004	0.008	0.006	0.006	0.012	0.011	0.002	0.016
Σ	4.997	4.997	4.997	4.991	5.009	5.002	5.011	4.996	5.007	4.992
An	60.78	62.09	58.84	61.31	55.89	57.46	55.34	57.66	54.06	55.02
Ab	38.72	37.11	40.76	37.88	43.52	41.90	43.49	41.24	45.74	43.36
Or	0.50	0.80	0.40	0.81	0.59	0.64	1.18	1.10	0.20	1.62

Sample:	KL14		KL10		r/cor	KL7		KL8			
	c	r	c	r		c	r	c	r	r*	spgy
SiO ₂	52.7	53.7	53.7	55.9	50.2	57.4	58.2	58.8	59.2	51.4	56.2
Al ₂ O ₃	29.3	29.3	28.8	26.9	30.9	26.4	25.4	25.7	25.4	30.3	26.7
CaO	12.2	12.0	11.2	9.44	14.2	8.53	7.84	7.33	7.43	13.3	9.29
FeO	0.07	0.37	0.08	0.31	0.45	0.09	0.16	0.12	0.24	0.39	0.52
Na ₂ O	4.55	4.48	5.05	5.62	3.26	6.59	6.74	7.08	6.86	3.74	5.71
K ₂ O	0.22	0.44	0.20	0.65	0.19	0.16	0.26	0.35	0.44	0.21	0.50
Total	99.04	100.18	99.06	98.78	99.22	99.23	98.61	99.35	99.55	99.41	98.94
Cations based on 8 oxygens											
Si	2.409	2.428	2.450	2.547	2.309	2.591	2.636	2.640	2.654	2.355	2.556
Al	1.581	1.560	1.547	1.444	1.676	1.407	1.358	1.362	1.343	1.634	1.433
Ca	0.599	0.580	0.547	0.461	0.699	0.412	0.381	0.353	0.357	0.653	0.453
Fe	0.003	0.014	0.003	0.012	0.017	0.003	0.006	0.005	0.009	0.015	0.020
Na	0.403	0.393	0.447	0.497	0.290	0.577	0.592	0.617	0.596	0.332	0.503
K	0.013	0.026	0.011	0.038	0.011	0.009	0.015	0.020	0.025	0.012	0.029
Σ	5.008	5.001	5.005	4.999	5.002	4.999	4.988	4.997	4.984	5.001	4.994
An	59.01	58.06	54.43	46.29	69.90	41.28	38.56	35.66	36.50	65.50	45.99
Ab	39.70	39.34	44.48	49.90	29.00	57.82	59.92	61.32	60.94	33.30	51.07
Or	1.28	2.60	1.09	3.81	1.10	0.90	1.52	2.02	2.56	1.20	2.94

¹c, r = core and rim analyses, respectively; r/cor = the rim of plagioclase mantling corundum grains; r* = the partially melted rim of plagioclase; spgy = 2nd plagioclase within spongy rim on Cpx.

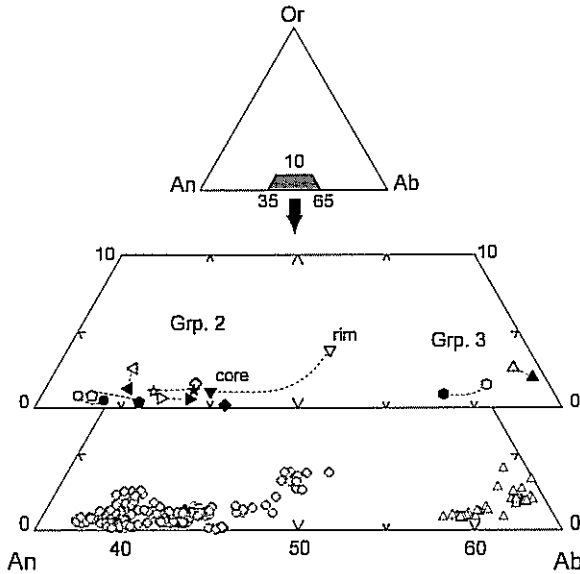
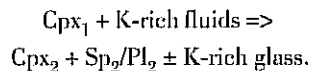


FIG. 8. Representative core and rim compositions of plagioclases shown with only selected tie-lines for clarity. Symbols in the upper quadrilateral are described in Figure 6. All analyses are also plotted in the lower quadrilateral to indicate compositional variations within each group. Open diamonds = group 2; open triangles = group 3.

compositions of kelyphite are similar to those of garnet precursors, but with slight increases in the Na_2O contents of kelyphite (up to 0.12%; Table 7). Such an increase is possibly balanced by a small decrease in Na as well as Ca and Al in rim analyses of the surrounding plagioclase and clinopyroxene, as evident in the Cpx compositional profile shown in Figure 7. Furthermore, kelyphite K_2O contents are undetectable, suggesting that chemical contribution from K-rich metasomatic fluids, such as those relating to the host basalts, was insignificant. Based on these observations, it is likely that kelyphite on garnets in the Thai granulite xenoliths are the result of metamorphic reaction between garnet and surrounding clinopyroxene and/or plagioclase. This kelyphitization was possibly developed upon decompression that occurred during the transportation of granulite xenoliths towards the Earth's surface (Rudnick, 1992; Obata, 1994). The relatively brief ascending time of these xenoliths may also have limited the progress of kelyphitization, resulting in the extremely fine grained nature of the kelyphite observed in this study.

Spongy-textured rinds or spongy rims are late-stage reaction textures developed on clinopyroxene, as the consequence of partial melting induced by

metasomatism (Taylor and Neal, 1989; Snyder et al., 1997b; Spetsius and Taylor, 2002). This partial melting involved the "leaching" of Na and Al from primary clinopyroxene (Cpx₁), and the formation of secondary phases in the spongy rims, characteristically between grain boundaries. In the present study, the spongy rims usually developed locally on the Cpx grains that are near the xenolith-host basalt interface, or on grains intersected by microfractures extending from the xenolith boundaries. This suggests that host basalts are the most likely sources of the K-rich fluids, which are required for the spongy rim formation. This is in contrast with the formation of kelyphite that occurs ubiquitously on all garnet grains in the xenoliths, with no evidence of metasomatic reaction. From this petrographic and geochemical evidence (Tables 4, 5, and 8), a reaction applicable to the Thai granulite xenoliths can be formulated as follows:



Snyder et al. (1997b) suggested that the intensity of this reaction is a function of the residence time of the xenolith in the host magma.

TABLE 6. Average Compositions of Garnet in Granulite Xenoliths¹

Sample: No. ²	KL9 8	KL5 11	KL12 15	KL13 10	KL11 12
SiO ₂	41.5 (3) ²	41.7 (1)	41.7 (1)	41.8 (1)	41.6 (3)
TiO ₂	0.04 (1)	0.04 (2)	0.04 (1)	0.06 (1)	0.04 (1)
Al ₂ O ₃	23.9 (1)	23.7 (2)	23.7 (1)	23.6 (2)	23.6 (1)
Cr ₂ O ₃	<0.03	0.03 (2)	0.09 (4)	<0.03	<0.03
MgO	19.8 (1)	18.2 (3)	18.1 (4)	17.6 (3)	17.2 (3)
CaO	4.77 (12)	8.00 (12)	6.94 (17)	8.50 (18)	8.27 (28)
MnO	0.20 (2)	0.13 (3)	0.20 (2)	0.14 (2)	0.16 (2)
FeO	9.97 (7)	7.95 (15)	9.45 (13)	8.36 (12)	9.25 (26)
Na ₂ O	<0.03	<0.03	<0.03	<0.03	<0.03
Total	100.28	99.81	100.27	100.00	100.07
Cations based on 12 oxygens					
Si	2.957	2.979	2.979	2.988	2.982
Ti	0.002	0.002	0.002	0.003	0.002
Al	2.005	1.997	1.995	1.990	1.992
Cr	0.001	0.002	0.005	0.001	0.001
Mg	2.103	1.943	1.928	1.872	1.840
Ca	0.364	0.612	0.531	0.651	0.636
Mn	0.012	0.008	0.012	0.009	0.010
Fe	0.594	0.475	0.564	0.500	0.555
Na	0.001	0.001	0.001	0.001	0.001
Σ	8.038	8.020	8.019	8.014	8.019
Pyr	68.4	64.0	63.5	61.7	60.5
Alm+Sps	19.7	15.9	19.0	16.8	18.6
Grs	11.8	20.2	17.5	21.5	20.9

¹Number of analyses of relic garnet cores used in the average.

²Represent 1 σ of replicate analyses in term of last unit cited.

P-T estimates

Granulite xenoliths that attained chemical and textural equilibrium, as indicated by compositional homogeneity among coexisting minerals and abundant triple-junction grain boundaries, were used for pressure-temperature estimates. These criteria, particularly mineral chemistry, render samples KL7, KL8, and KL14 useless for P-T estimations, because the clinopyroxenes are strongly zoned (Fig. 7). For suitable samples, only core compositions of primary minerals were used to avoid secondary products developed at rims of the primary minerals or along grain boundaries. P-T estimates obtained from the cores, therefore, represent the last equi-

libration conditions prior to the development of these secondary textures. All P-T calculations were carried out using several mineral pairs in a given sample.

Using a number of Cpx-Gt thermometers (at 15 kbar reference pressure), temperature estimates from the granulite xenoliths in Thailand are approximately 1100–1200°C (Table 10). The thermometers used here are relatively insensitive to pressure changes, consistent with observations in previous studies (Pearson et al., 1991, 1995). For instance, temperature calculations using reference pressures of 10 and 20 kbar result in only $\pm 20^\circ\text{C}$ variations from those at 15 kbar pressure. Generally, Ellis and Green (1979) temperature estimates (1095–1193°C)

TABLE 7. Average Compositions of Kelyphite in Granulite Xenoliths¹

Sample: No. ²	KL9 15	KL5 17	KL12 18	KL13 19	KL11 23	KL4a 31	KL7 8
SiO ₂	41.8 (3) ³	41.7 (4)	41.8 (4)	41.8 (3)	41.7 (2)	41.5 (3)	40.5 (3)
TiO ₂	0.03 (1)	0.04 (1)	0.04 (1)	0.05 (1)	0.03 (1)	0.04 (2)	0.13 (1)
Al ₂ O ₃	23.7 (2)	23.7 (2)	23.7 (3)	23.5 (3)	23.6 (2)	23.6 (4)	22.7 (3)
Cr ₂ O ₃	0.03 (2)	<0.03	0.13 (4)	0.04 (2)	<0.03	0.08 (4)	0.08 (2)
MgO	19.7 (2)	18.0 (5)	17.6 (4)	17.3 (4)	17.0 (3)	17.0 (8)	12.6 (3)
CaO	4.53 (25)	7.93 (26)	7.04 (27)	8.37 (27)	8.16 (31)	7.80 (61)	7.32 (41)
MnO	0.20 (3)	0.14 (3)	0.20 (3)	0.15(2)	0.16 (2)	0.16 (2)	0.40 (3)
FeO	9.87 (14)	7.91 (13)	9.37 (18)	8.31 (22)	9.14 (26)	9.09 (41)	15.3 (6)
Na ₂ O	0.12 (9)	0.10 (6)	0.09 (4)	0.06 (6)	0.06 (5)	0.07 (6)	0.07 (4)
K ₂ O	<0.03	<0.03	<0.03	<0.03	<0.03	<0.03	<0.03
Total	99.96	99.53	99.91	99.50	99.87	99.43	99.17

¹"Bulk" kelyphite analyses were obtained using a 10 μm beam.

²Number of analyses used in the average.

³Represent 1 σ of replicate analyses in term of last unit cited.

TABLE 8. Representative Analyses of Spinel¹

Sample:	KL9	KL10 spgy	KL10 r/cor
SiO ₂	0.04	0.03	0.06
TiO ₂	<0.03	<0.03	0.09
Al ₂ O ₃	66.0	66.4	65.7
Cr ₂ O ₃	0.41	0.04	0.04
MgO	21.3	21.2	16.1
MnO	<0.03	0.03	0.20
FeO	11.4	11.6	17.2
NiO	0.33	0.42	0.12
ZnO	0.14	0.09	0.05
Total	99.58	99.82	99.61
Cations based on 4 oxygens			
Si	0.001	0.001	0.001
Ti	0.000	0.000	0.002
Al	1.958	1.965	1.996
Cr	0.008	0.001	0.001
Mg	0.800	0.795	0.619
Mn	0.000	0.001	0.004
Fe	0.239	0.243	0.372
Ni	0.007	0.009	0.003
Zn	0.003	0.002	0.001
Σ	3.016	3.017	2.999
Mg#	77.0	76.6	62.5

¹spgy = 2nd spinel within spongy rim on Cpx; r/cor = rim of spinel that surrounds corundum core.

are in good agreement with those of Powell (1985)(1088–1194°C), whereas the largest differences occur between those from Ganguly (1979) and Krogh (1988) thermometers (1124–1184°C and 1043–1223°C, respectively). The maximum temperature difference (±44°C) observed in KL9 is possibly due to the low grossular content of garnet that affects the partitioning of Fe²⁺ and Mg in both garnet and clinopyroxene (Krogh, 1988).

Equilibration pressures were obtained from the barometer of Eckert et al. (1991), using average temperatures. This barometer is calibrated from the assemblage Cpx-Gt-Pl-Qtz and is essentially a modification of the Newton and Perkins (1982) barometer. It is obvious from this and other studies (e.g., Pearson et al., 1991) that this barometer is relatively insensitive to temperature changes. That is, a variation of ~100°C results in a change of only 1 kbar, which is well within the precision of this barometer (±1.90 kbar). Calculations using mineral compositions of the Thai granulite xenoliths yield a small pressure range of ~15 to 18 kbar (Table 10). Pressure cannot be estimated for Ol-Gt clinopyroxenite KL9 due to the absence of plagioclase.

The pressure estimates of 15–18 kbar translate to depths of ~50–60 km (assuming 3.3 km = 1 kbar). If the granulite xenoliths represent lower crustal fragments, these depths suggest relatively thick crust in a region that had experienced recent basalt volcanism (Kopylova et al., 1995). Alternatively,

TABLE 9. Average Compositions of Olivine and Corundum¹

Sample:	KL9 Ol (4) ²		KL5 Cor (15)	KL10 Cor (14)	KL13 Cor (9)
SiO ₂	39.9 (3) ³	TiO ₂	0.03 (1)	<0.03 (2)	0.04 (0)
MgO	46.8 (4)	Al ₂ O ₃	98.8 (3)	99.6 (6)	99.3 (4)
CaO	0.06 (1)	Cr ₂ O ₃	0.20 (10)	0.04 (2)	0.03 (2)
MnO	0.09 (2)	Fe ₂ O ₃ ⁴	0.62 (7)	0.49 (13)	0.46 (10)
FeO	13.1 (0)	MgO	0.03 (1)	0.03 (1)	0.03 (0)
NiO	0.26 (4)				
Total	100.25	Total	99.63	100.18	99.85
O-basis:	4		3	3	3
Si	0.992	Ti	0.000	0.000	0.001
Mg	1.734	Al	1.991	1.992	1.993
Ca	0.002	Cr	0.003	0.001	0.000
Mn	0.002	Fe	0.008	0.006	0.005
Fe	0.273	Mg	0.001	0.001	0.001
Ni	0.005				
Σ	3.008	Σ	2.001	2.000	2.000
Fo	86.38				

¹Abbreviations: Ol = olivine; Cor = corundum.

²Number of analyses used in the average.

³Represent 1 σ of replicate analyses in term of last unit cited.

⁴Fe is analyzed as Fe₂O₃.

these granulites could have been derived from mafic lenses that intruded into the upper mantle wall rock (Chen et al., 2001). In a broad sense, it can be inferred that these granulite xenoliths represent the lower continental crust at the crust-mantle transition zone.

Formation of corundum inclusions

Unraveling the origin of gem-quality corundum in the region of Thailand has been a major goal of several investigations (e.g., Coenraads et al., 1995; Levinson and Cook, 1995; Guo et al., 1996; Sutherland et al., 1998; Limtrakun et al., 2001; Suthirath et al., 2001). Despite these efforts, however, there is still no consensus regarding the genesis of these gem-quality corundum megacrysts, partly because of the apparent absence of corundum-bearing rocks that could provide detailed petrogenetic information. Our corundum-bearing granulite xenoliths may represent this missing information. However, there are apparently different modes of origin for corundum inclusions and gem-corundum megacrysts, so

we limit our interpretations to the formation of corundum inclusions in granulite xenoliths. Nevertheless, our corundum-bearing xenoliths place constraints on the conditions at which corundum crystallized, and are potentially useful for future efforts to understand the genesis of these gemstones.

In this study, corundum occurs as inclusions in three granulite xenoliths of the garnet-rich group (KL5, KL10, and KL13), but is distributed heterogeneously in the studied thin sections. These inclusions are observed only within plagioclase and kelyphite hosts (Figs. 2B and 2C); none has been found in clinopyroxene or olivine, or as discrete grains. Moreover, corundum is typically surrounded by spinel rims, and, in some cases, by intermediate rims of spinel and outermost rims of plagioclase.

High-pressure metamorphism has been used to explain the formation of corundum in some mafic rocks. Kornprobst et al. (1990) interpreted corundum in garnet clinopyroxenites from Beni Bousera, Morocco as the product of high-pressure metamorphism of basaltic-cumulate protoliths that contained

TABLE 10. Temperature and Pressure Estimates of Granulite Xenoliths from Thailand¹

Sample:	T (°C)						P (kbar) E91
	EG79	G79	P85	K88	Avg.	S.D.	
KL9	1110	1152	1093	1043	1097	44	—
KL12	1095	1124	1088	1085	1098	18	15.5
KL11	1162	1158	1161	1190	1168	15	18.0
KL13	1188	1174	1188	1223	1193	21	18.1
KL5	1193	1184	1194	1223	1199	17	18.3

¹EG79 = Ellis and Green, 1979; G79 = Ganguly, 1979; P85 = Powell, 1985; K88 = Krogh, 1988; E91 = Eckert et al. (1991). Temperature estimates were calculated at a pressure of 15 kbar reference pressure. Pressures were calculated using average temperatures.

Cpx, Ol, and Pl. Similarly, Morishita and Arai (2001) stated that corundum in mafic rocks from the Horoman peridotite complex in Japan formed by the reaction: spinel + anorthite = 2 corundum + diopside, which occurred at >15 kbar and at 1000°C. Corundum inclusions described in the present study may have formed by such a metamorphic process. However, it is difficult to explain the exclusive occurrence of corundum as inclusions but never as discrete grains, as occurs in the aforementioned studies.

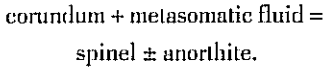
Corundum inclusions in plagioclase can be the result of Al₂O₃ exsolving from a plagioclase host at elevated pressures and temperatures (> 9 kbar and 1200°C; Goldsmith, 1980). This corundum exsolution, then, results in non-stoichiometric or Al₂O₃-deficient anorthite with site vacancies. This process, however, may not be applicable to this study, inasmuch as EMP analyses, apparently, suggest stoichiometric anorthite in all studied Cor-bearing granulite xenoliths (Table 5).

Partial melting of Al-rich mafic rocks at high temperatures and pressures also produces corundum as a liquidus phase (e.g., Råheim and Green, 1974; Presnall et al., 1978; Milholland and Presnall, 1998). Plagioclase melts incongruently at high pressures, i.e., > 10 kbar, producing corundum crystals (Boyd and England, 1961; Hariya and Kennedy, 1968; Presnall et al., 1978). This partial melting of plagioclase-bearing rocks at elevated pressures seems consistent with the presence of corundum inclusions within stoichiometric plagioclases, and with the high P-T history (i.e., ~1190°C and 18 kbar) of the corundum-bearing samples (KL13 and KL5). The rare occurrence of corundum in these

samples suggests that partial melting of the granulite xenoliths or their protoliths must have been within the lower crust, limited in extent, and with no significant amount of melt being extracted. Possibly, the melting that resulted in the corundum formation is a late-stage process relating to basaltic magmatism that eventually brought granulite xenoliths to the surface. This scenario is in agreement with the whole-rock chemistry, particularly REEs, which has largely preserved the protolith signature. It is unclear, however, if this partial melting occurred in the Ol-Pl-Cpx protoliths or after the transformation to the garnet granulites, because both rock types contain plagioclase that could have melted incongruently. Inasmuch as corundum inclusions are also found in kelyphitized garnets, it can be inferred that some plagioclases already contain corundum inclusions prior to their complete transformation to garnets. Although corundum inclusions were not observed in unaltered garnet grains, this is probably due to the rare occurrences of corundum inclusions, and the consistency of kelyphitization that occurred on all garnet grains.

In sample KL10, many corundum inclusions appear to have been reacted to spinel, and, in a few cases, to spinel ± plagioclase rims (Fig. 2C). In contrast, corundum inclusions in KL5 are in direct contact with kelyphite, without any reaction texture. Thus, it is possible that these rims are the product of reaction between corundum and external components, possibly metasomatic fluids related to the host basalt. The abundant occurrences of spongy rims on Cpx in granulite KL10 are consistent with this interpretation. Morishita and Arai (2001; and references therein) proposed a possible reaction of

corundum disappearance: $2 \text{ corundum} + \text{diopside} = \text{spinel} + \text{anorthite}$. Applied to this study, this reaction could be written as:



There is an apparent correlation between the Al content in Cpx and the presence of corundum in granulite xenoliths. As demonstrated in Figure 6, corundum only occurs in the samples in which clinopyroxene contains at least ~14 wt% Al_2O_3 . Occurrences of corundum in mafic rocks elsewhere are consistent with this observation. Based on P-T estimates obtained in this study, it can be inferred that corundum in mafic rocks crystallized at a minimum temperature and pressure of approximately 1190°C and 18 kbar.

Conclusions

Mineralogical and geochemical evidence suggests that the granulite xenoliths from the Chantaburi province of Thailand were derived from basaltic cumulate protoliths similar to troctolite and olivine gabbro. Subsidiary re-equilibration later transformed these cumulate protoliths to granulite-facies lithologies by forming garnet and clinopyroxene at the expense of plagioclase and olivine. P-T estimates indicate that the granulite xenoliths were last equilibrated at ~1100–1200°C and 15–18 kbar, consistent with lower-crustal/upper-mantle depths of approximately 50 to 60 km. Interestingly, the upper limit of this P-T range (i.e., $\geq 1190^\circ\text{C}$, 18 kbar) marks the appearance of corundum inclusions that coexist with clinopyroxene in which Al_2O_3 contents are ≥ 14 wt%. These corundum inclusions possibly formed by incongruent melting of plagioclase as a result of a brief, late-stage partial melting period, which possibly occurred prior to the completion of the granulite-facies metamorphism. Although the timing of igneous and metamorphic events involved in the formation of granulite xenoliths cannot be constrained by the present study, based on the radiometric-dating data of Thai basalts (0.6–9 Ma; see references in Promprated et al., 1999), it is reasonable to infer that granulite-forming events are Late Cenozoic phenomena.

Granulite xenoliths observed in this study provide direct evidence for the presence of mafic lower crust beneath Thailand. It is possible that the gener-

ation of this lower crust was a consequence of underplating during prolonged periods of basaltic magmatism in the Late Cenozoic, which eventually erupted and brought up gem-quality corundum megacrysts.

Acknowledgements

We are grateful to Allan Patchen for assistance with the EMP analyses, and to Jinesh Jain for help in obtaining the ICP-MS data. Comments on the earlier version of the manuscript from Mahesh Anand are appreciated. Rak Hansawek and Yaowaluck Api-chatachutapan provided logistic supports during field work, for which we appreciate. This research was in part funded by NSF grants EAR 97-25885 and EAR 99-09430 to LAT.

REFERENCES

- Anders, E., and Grevesse, N., 1989, Abundances of the elements: Meteoritic and solar: *Geochimica et Cosmochimica Acta*, v. 53, p. 197–214.
- Barr, S. M., and Dostal, J., 1986, Petrochemistry and origin of megacrysts in Upper Cenozoic basalts, Thailand: *Journal of Southeast Asian Earth Sciences*, v. 1, p. 107–116.
- Barr, S. M., and MacDonald, A. S., 1978, Geochemistry and petrogenesis of late Cenozoic alkaline basalts of Thailand: *Geological Society of Malaysia, Bulletin*, v. 10, p. 25–52.
- _____, 1981, Geochemistry and geochronology of late Cenozoic basalts of Southeast Asia: *Geological Society of America Bulletin*, v. 92, p. 1069–1142.
- Benoit, M., Polvé, M., and Ceulener, G., 1996, Trace element and isotopic characterization of mafic cumulates in a fossil mantle diapir (Ornan ophiolite): *Chemical Geology*, v. 134, p. 199–214.
- Boyd, F. R., and England, J. L., 1961, Melting of silicates at high pressures: *Carnegie Institution of Washington, Yearbook*, v. 60, p. 113–125.
- Bunopas, S., and Vella, P., 1992, Geotectonic and geologic evolution of Thailand, in *Proceedings of National Conference on the Geological Resources of Thailand: Potential for Future Development*: Bangkok, Thailand, Department of Mineral Resources, Thailand, p. 209–228.
- Chen, S., O'Reilly, S. Y., Zhou, X., Griffin, W. L., Zhang, G., Sun, M., Feng, J., and Zhang, M., 2001, Thermal and petrological structure of the lithosphere beneath Hannuoba, Sino-Korean Craton, China: Evidence from xenoliths: *Lithos*, v. 56, p. 267–301.
- Coenraads, R. R., Vichit, P., and Sutherland, F. L., 1995, An unusual sapphirine-zircon-magnetite xenolith from

- the Chanthaburi gem province, Thailand: *Mineralogical Magazine*, v. 59, p. 465–479.
- Eckert, J. O., Jr., Newton, R. C., and Kleppa, O. J., 1991, The ΔH of reaction and recalibration of garnet-pyroxene-plagioclase-quartz geobarometers in the CAMS system by solution calorimetry: *American Mineralogist*, v. 76, p. 148–160.
- Ellis, D. J., and Green, D. H., 1979, An experimental study of the effect of Ca upon garnet-clinopyroxene Fe-Mg exchange equilibria: *Contributions to Mineralogy and Petrology*, v. 71, p. 13–22.
- Ganguly, J., 1979, Garnet and clinopyroxene solid solution, and geothermometry based on Fe-Mg distribution coefficient: *Geochimica et Cosmochimica Acta*, v. 43, p. 1021–1029.
- Garvie, O. G., and Robinson, D. N., 1984, The formation of kelyphite and associated sub-kelyphitic and sculptured surfaces on pyrope from kimberlite, in Kornprobst, J., *Kimberlites I: Kimberlites and related rocks*, v. 11A: Amsterdam, Netherlands, Elsevier, p. 371–382.
- Goldsmith, J. R., 1980, The melting and breakdown reactions of anorthite at high pressures and temperatures: *American Mineralogist*, v. 65, p. 272–284.
- Griffin, W. L., and O'Reilly, S. Y., 1986, The lower crust in eastern Australia: Xenolith evidence, in Dawson, J. B., Carswell, D. A., Hall, J., Wedepohl, K. H., eds., *The nature of the lower continental crust: Geological Society of London Special Publication*, v. 24, p. 363–374.
- Guo, J., O'Reilly, S. Y., and Griffin, W. L., 1996, Corundum from basaltic terrains: A mineral inclusion approach to the Enigma: *Contributions to Mineralogy and Petrology*, v. 122, p. 368–386.
- Hariya, Y., and Kennedy, G. C., 1968, Equilibrium study of anorthite under high pressure and high temperature: *American Journal of Science*, v. 266, p. 193–202.
- Harley, S. L., 1989, The origin of granulites: A metamorphic perspective: *Geological Magazine*, v. 126, p. 215–331.
- Hunter, R. H., and Taylor, L. A., 1982, Instability of garnet from the mantle: Glass as evidence of metasomatic melting: *Geology*, v. 10, p. 617–620.
- Intasopa, S., Alichat, W., Pisutha-Arnond, V., Sriprasert, B., Narudeesombat, N., and Puttharat, T., 1999, Inclusions in Chanthaburi-Trat corundums: A clue to their genesis, in *Proceedings of the Conference on the Mineral, Energy, and Water Resources of Thailand: Towards the Year 2000*, p. 471–584 (in Thai).
- Jezek, D. A., Sinton, J. M., Jarosewich, E., and Obermeyer, C. R., 1978, Fusion of rock mineral powders for electron microprobe analysis: *Smithsonian Contributions to Earth Sciences*, v. 22, p. 46–52.
- Kopylova, M. G., O'Reilly, S. Y., and Genshaft, Y. S., 1995, Thermal state of the lithosphere beneath Central Mongolia: Evidence from deep-seated xenoliths from Shavaryn-Saram volcanic center in Tariat depression, Hangai, Mongolia: *Lithos*, v. 36, p. 243–255.
- Kornprobst, J., Piboule, M., Roden, M., and Tabit, A., 1990, Corundum-bearing garnet clinopyroxenites at Beni Bousera (Morocco): Original plagioclase-rich gabbros recrystallized at depth within the mantle: *Journal of Petrology*, v. 31, p. 717–745.
- Krogh, E. J., 1988, The garnet-clinopyroxene Fe-Mg geothermometer—A reinterpretation of existing experimental data: *Contributions to Mineralogy and Petrology*, v. 99, p. 44–48.
- Kushiro, I., and Yoder, Jr., H. S., 1966, Anorthite-forsterite and anorthite-enstatite reactions and their bearing on basalt-eclogite transformation: *Journal of Petrology*, v. 7, p. 337–362.
- Levinson, A. A., and Cook, F. A., 1995, Gem corundum in alkali basalt: Origin and occurrence: *Gems and Gemology*, v. 30, p. 253–262.
- Limtrakun, P., Zaw, K., Ryan, C. G., and Mernagh, T. P., 2001, Formation of the Denchai sapphires, northern Thailand: Evidence from mineral chemistry and fluid/melt inclusion characteristics: *Mineralogical Magazine*, v. 65, p. 725–735.
- Liu, Y. S., Gao, S., Jin, S. Y., Hu, S. H., Sun, M., Zhao, Z. B., and Feng, J. A., 2001, Geochemistry of lower crustal xenoliths from Neogene Hannuoba basalt, North China Craton: Implications for petrogenesis and lower crustal composition: *Geochimica et Cosmochimica Acta*, v. 65, p. 2589–2604.
- Loock, G., Stosch, H.-G., and Seck, H.A., 1990, Granulite facies lower crustal xenoliths from the Eifel, West Germany: Petrological and geochemical aspects: *Contributions to Mineralogy and Petrology*, v. 105, p. 25–41.
- Millholland, C. S., and Presnall, D. C., 1998, Liquidus phase relations in the CaO-MgO-Al₂O₃-SiO₂ system at 3.0 GPa: The aluminous pyroxene thermal divide and high-pressure fractionation of picritic and komatiitic magmas: *Journal of Petrology*, v. 39, p. 3–27.
- Morishita, T., and Arai, S., 2001, Petrogenesis of corundum-bearing mafic rock in the Horoman peridotite complex, Japan: *Journal of Petrology*, v. 42, p. 1279–1299.
- Mukasa, S. M., Fischer, G. M., and Barr, S. M., 1996, The character of the subcontinental mantle in Southeast Asia: Evidence from isotopic and elemental compositions of extension-related Cenozoic basalts in Thailand, in Basu, A. R., and Hart, S. R., eds., *Earth processes: Reading the isotope code: American Geophysical Union, Geophysical Monograph 95*, p. 233–252.
- Neal, C. R., 2001, The interior of the Moon: The presence of garnet in the primitive, deep lunar mantle: *Journal of Geophysical Research*, v. 106, p. 27,865–27,885.
- Newton, R. C., and Perkins, D., III, 1982, Thermodynamic calibration of geobarometers based on assemblages garnet-plagioclase-orthopyroxene (clinopyroxene)-quartz: *American Mineralogist*, v. 67, p. 203–222.

- Obata, M., 1994, Material transfer and local equilibria in a zoned kelyphite from garnet pyroxenite, Ronda, Spain: *Journal of Petrology*, v. 35, p. 271–287.
- Pearson, N. J., O'Reilly, S. Y., and Griffin, W. L., 1991, The granulite to eclogite transition beneath the eastern margin of the Australian craton: *European Journal of Mineralogy*, v. 3, p. 293–322.
- _____, 1995, The crust-mantle boundary beneath cratons and craton margins: A transect across the southwest margin of the Kaapvaal craton, *Lithos*, v. 36, p. 257–287.
- Powell, R., 1985, Regression diagnostics and robust regression in geothermometer/geobarometer calibration: The garnet-clinopyroxene geothermometer revisited: *Journal of Metamorphic Geology*, v. 3, p. 231–243.
- Presnall, D. C., Dixon, S. A., O'Donnell, T. H., Brenner, N. L., Schrock, R. L., and Dycus, D. W., 1978, Liquidus phase relations on the join diopside-forsterite-anorthite from 1 atm to 20 kbar: Their bearing on the generation and crystallization of basaltic magma: Contributions to Mineralogy and Petrology, v. 66, p. 203–220.
- Promprated, P., Taylor, L. A., and Snyder, G. A., 1999, Petrochemistry of the mantle beneath Thailand: Evidence from peridotite xenoliths: *International Geology Review*, v. 41, p. 506–530.
- Qi, Q., Taylor, L. A., Snyder, G. A., Clayton, R. N., Mayeda, T. K., and Sobolev, N. V., 1997, Detailed petrology and geochemistry of rare corundum eclogite xenoliths from Obnazhennaya, Yakutia: *Russian Geology and Geophysics*, v. 38, p. 247–260.
- Råheim, A., and Green, D. H., 1974, Experimental petrology of lunar highland basalt composition and application to models for the lunar interior: *Journal of Geology*, v. 82, p. 607–622.
- Rogers, N. W., and Hawkesworth, C. J., 1982, Proterozoic age and cumulate origin for granulite xenoliths, Lesotho: *Nature*, v. 299, p. 409–413.
- Rudnick, R. L., 1992, Xenoliths—Samples of the lower continental crust, in Fountain, D. M., Arculus, R., and Kay, R. W., eds., *Continental lower crust*: Amsterdam, Netherlands, Elsevier, p. 269–316.
- Rudnick, R. L., and Fountain, D. M., 1995, Nature and composition of the continental: A lower crustal perspective: *Reviews in Geophysics*, v. 33, p. 267–309.
- Rudnick, R. L., McDonough, W. F., McCulloch, M. T., and Taylor, S. R., 1986, Lower crustal xenoliths from Queensland, Australia: Evidence for deep crustal assimilation and fractionation of continental basalts: *Geochimica et Cosmochimica Acta*, v. 50, p. 1099–1115.
- Salyaphongse, S., and Jungyusuk, N., 1983, Geological map of Thailand 1:500,000, Central and Eastern sheet: Bangkok, Thailand, Geological Survey Division, Department of Mineral Resources.
- Sivabovorn, V., Paichitprapaporn, V., and Tansulein, S., 1976, *Geology of Phratabong-Chanthaburi* (Sheet ND 48-9, ND48-13): Bangkok, Thailand, Geological Survey Division, Department of Mineral Resources, Report, 51 p. (in Thai).
- Snyder, G. A., Taylor, L. A., Crozaz, G., Halliday, A. N., Beard, B. L., Sobolev, V. N., and Sobolev, N. V., 1997a, The origins of Yakutian eclogite xenoliths: *Journal of Petrology*, v. 38, p. 85–113.
- Snyder, G. A., Taylor, L. A., Jin, Y., and Taylor, D.-H., 1997b, Mantle-lherzolite xenoliths from eastern China: Petrogenesis and development of secondary texture: *International Geology Review*, v. 39, p. 671–687.
- Sobolev, V. N., Taylor, L. A., and Snyder, G. A., 1994, Diamondiferous eclogites from the Udachnaya kimberlite pipe, Yakutia: *International Geology Review*, v. 36, p. 42–64.
- Spetsius, Z. V., and Taylor, L. A., 2002, Partial melting in mantle xenoliths: Connections with diamond paragenesis: *International Geology Review*, v. 44, p. 973–987.
- Stosch, H.-G., Ionov, D. A., Puchtel, I. S., Galer, S. J. G., and Sharpouri, A., 1995, Lower crustal xenoliths from Mongolia and their bearing on the nature of the deep crust beneath central Asia: *Lithos*, v. 36, p. 227–242.
- Sutherland, F. L., Hoskin, W. O., Fanning, C. M., and Coenraads, R. R., 1998, Models of corundum origin from alkali basaltic terrains: A reappraisal: Contributions to Mineralogy and Petrology, v. 133, p. 356–372.
- Sutthirat, C., Saminpanya, S., Droop, G. T. R., Henderson, C. M. B., and Manning, D. A. C., 2001, Clinopyroxene-corundum assemblages from alkali basalt and alluvium, eastern Thailand: Constraints on the origin of Thai rubies: *Mineralogical Magazine*, v. 65, p. 277–295.
- Taylor, L. A., and Neal, C. R., 1989, Eclogites with oceanic crustal and mantle signatures from the Bellsbank kimberlite, South Africa, part 1: Mineralogy, petrography, and whole-rock chemistry: *Journal of Geology*, v. 97, p. 551–567.
- Thompson, A. B., 1979, Metamorphism in a model mantle: I. Predictions of *P-T-X* relations in CaO-Al₂O₃-MgO-SiO₂, in Boyd, F. R., and Meyer, H. O. A., eds., *The mantle samples: Inclusions in kimberlites and other volcanics*: Proceedings of the International Kimberlite Conference, v. 2: Washington, DC, American Geophysical Union, p. 15–28.
- Vichit, P., 1992, Gemstones in Thailand, in Proceedings of National Conference on the Geological Resources of Thailand: Potential for future development: Bangkok, Thailand, Department of Mineral Resources, Thailand, p. 124–150.
- Vichit, P., Vudchichativanich, S., and Hansawek, R., 1978, The distribution and some characteristics of corundum-bearing basalts in Thailand: *Journal of the Geological Society of Thailand* (special issue for III GEOSEA), v. 3, no. 4, p. 1–38.

Wohletz, K., 1996, Magna2 (software) [<http://geonl.lanl.gov/Wohletz/Wohletz.htm#Software>].

Zang, Q., Enami, M., and Suwa, K., 1993, Aluminian orthopyroxene in pyrometamorphosed garnet mega-

crysts from Liaoning and Shandong provinces, north-east China: *European Journal of Mineralogy*, v. 5, p. 153–164.